



STOCHASTIC CONDITIONAL SIMULATION OF AFTERSHOCK ACCELEROGRAMS GIVEN THE PARENT MAIN SHOCK

S. Das⁽¹⁾, V.L. Nithin⁽²⁾, H.B. Kaushik⁽³⁾

⁽¹⁾Assistant Professor, Department of Civil Engineering, IIT Guwahati, India, sandip.das@iitg.ac.in

⁽²⁾Graduate Student, Department of Civil Engineering, IIT Guwahati, India, nithin.l@iitg.ac.in

⁽³⁾Professor, Department of Civil Engineering, IIT Guwahati, India, hemanthk@iitg.ac.in

Abstract

The importance of aftershocks in seismic design is somewhat underrated. Various codes of practice in different countries still do not have any clear provision on how to make a structure safe enough so that it can withstand the likely aftershocks after it survives the main shock. It has been learnt from several recent major earthquakes that structures after surviving the main shock can eventually collapse during aftershocks. It is imperative to have detailed nonlinear time-history analysis (NTHA) of damaged buildings (during the main event) under aftershock ground motions before proposing any design recommendation. However, sufficient recorded main shock aftershock sequences for any given seismological scenario are not available. In order to cater to this need various methods of forming main shock aftershock sequences are proposed by many researchers in the recent past. These methods range from considering randomized motion after uniform scaling as an aftershock to considering motion by addressing the dependence of aftershock ground motion features (e.g., frequency content, duration) on the preceding main shock. The dependence is usually accomplished by considering some as-recorded aftershock motions with similar seismic scenario as the anticipated/targeted one. It is however not possible in this way to get as many aftershock ground motions as needed (for statistical estimate through NTHA) with desired inherent variability while all of them as a whole satisfy the dependency on their parent main shock. Such an overall dependency in statistical sense is crucial because NTHA is in general highly sensitive to the time-frequency characteristics of a ground motion. Currently there is no method available to form a suite of main shock aftershock sequences where the main shock motion is given along with any anticipated/targeted seismological scenario for the future aftershock. In this paper a stochastic simulation method is proposed to get a suite of aftershock ground motions conditionally obtained from the given main shock ground motion such that they satisfy the stochastic dependence of their time-frequency characteristics on their parent main shock vis-à-vis the seismological disparities between the main shock and the aftershock. The current proposition has two parts, viz., i) time-efficient stochastic simulation of samples from frequency-dependent instantaneous energy arrival (FDIEA) of decomposed time-histories and ii) conditional estimates of FDIEA for an aftershock from given FDIEA for the parent main shock via regression analysis using the disparities among the seismological parameters of the main shock and its aftershock. It is found that a conditionally obtained FDIEA of aftershock yields samples of aftershock ground motions that are better in terms of capturing the observed dependence on the preceding main shock as compared to the samples of aftershock when the FDIEA is estimated unconditionally from the corresponding seismological parameters of the aftershock. Hence, the present work will facilitate the much-needed comprehensive study on statistically significant trend of additional damage causing ability of aftershocks vis-à-vis seismological scenarios for meaningful design recommendations.

Keywords: conditional simulation; main shock aftershock sequence; energy arrival; decomposed time-history



1. Introduction

Time-history analysis (THA) is essential to carry out detailed nonlinear analysis of structures to perform stochastic investigation of response quantities [1]. Response statistics requires ensemble of ground motions as input, which is not possible to get in recorded form for a desired scenario. So researchers often consider recorded motions corresponding to different seismic scenarios before suitably scaling them to fulfill their needs [2–4]. Recently a few researchers have proposed methodologies to get scenario-specific nonstationary ground motions to cater to the need of statistical analysis [5–7]. The nonlinear THA for main shock-aftershock sequence is more involved than that for an individual event scenario. Because, despite aftershocks being independent entities, their characteristics are believed to be correlated with those of the preceding main shock [8–10]. In fact, such a dependence can be accounted for at the spectrum or the strong motion duration (SMD) level with disparities of the seismological parameters for main shock and its aftershock [8]. However, several researchers consider randomized (simulated) main shock-aftershock ground motion sequences for simplicity. Goda [11,12] has shown that the nonstationary features of the recorded aftershocks are very much critical for proper response statistics and a randomized sequence strategy may be faulty. Recently, Papadopoulos et al. [10] has shown the existence of significant correlation between spectral acceleration residuals of main shocks and their aftershocks.

Sigma oscillatory process (summation of individual Priestley processes) is more general than the ordinary Priestley oscillatory process in the case of a multivariate random process [13,14]. However, for univariate process simulation, as in the present case, Priestley process assumption is sufficient. Recently, Nithin et al. [7] has proposed a Priestley process based stochastic simulation of ground motions from a given seismic scenario through scaling model of frequency-dependent instantaneous energy arrival (FDIEA) curves, which fully govern the nonstationary features. This method is applicable for aftershock motion simulation but only unconditionally, i.e., independent of the parent (known) main shock. Hu et al. [15] has proposed a method for aftershock ground motions simulation, which does not explicitly consider the dependence on the preceding main shock. Das and Gupta [16] has shown that one sample of aftershock can be simulated from the recorded parent main shock motion for given SMD and pseudo spectral acceleration for the aftershock, where the frequency-wise envelopes of the main shock sample are replicated (with uniform shrinking or scaling) into the aftershock sample. So, this method is not favourable for ensemble simulation of aftershock motions with desired variability of their nonstationary pattern. Therefore, it is necessary to develop a method for statistical simulation of aftershock motions from the known main shock at a site and from the knowledge of the seismic scenario of the anticipated aftershock. In the current study, a Priestley process-based framework for aftershock simulation is proposed where the nonstationarities of the anticipated aftershock motion are characterized from that of the recorded main shock at the same site. For this purpose, a conditional scaling model for the FDIEA curves of the aftershock is newly proposed and the process-specific samples generation method proposed earlier by Nithin et al. [7] has been improved for direct and faster ground motion simulation. The database of main shock and aftershock ground motions recorded during 1999 Chi-Chi earthquake has been used for development of scaling relationships.

2. Stochastic Process-Specific Ground Motion Simulation

The characterization of a recorded ground motion process is based on the method due to Nithin et al. [7]. The method utilizes FDIEA curves of the modified L-P wavelet coefficients [17] of different frequency bands in order to extract the frequency-wise amplitude modulation for Priestley process representation. This method is first briefly reviewed because a similar method is proposed in decomposed (frequency band-wise) time-history domain as opposed to the wavelet-domain. This is done because the amplitude modulations for Priestley process can also be extracted from the decomposed time-histories with equal efficiency and the latter give faster reconstruction of motion than the wavelet coefficients.



2.1 Review of Wavelet-based Simulation

The wavelet coefficient of a ground motion record $f(t)$ is expressed as

$$W_{\psi}f(a, b) = \langle f, \psi_{a,b} \rangle = \int_{-\infty}^{\infty} f(t)\psi_{a,b}(t)dt \quad (1)$$

where, $\psi_{a,b}(t)$ is the real wavelet basis with a dilation parameter $a > 0$ and a shift parameter b given as

$$\psi_{a,b}(t) = \frac{1}{a^{1/2}}\psi\left(\frac{t-b}{a}\right) \quad (2)$$

where, $\psi(t)$ is called the mother wavelet. In the present study, the modified L-P wavelet basis is used, for which the mother wavelet is defined as

$$\psi(t) = \frac{1}{\pi\sqrt{\sigma-1}} \frac{\sin(\sigma\pi t) - \sin(\pi t)}{t} \quad (3)$$

with σ taken as $2^{1/4}$ [17]. The dilation parameter a is further discretized into 32 different levels by taking $a_j = \sigma^j$ such that different levels, indexed by j , correspond to different narrow frequency bands. Hence, the wavelet coefficients for a particular level, j , can be expressed as

$$W_{\psi}f(a_j, b) = \langle f, \psi_{a_j,b} \rangle = \int_{-\infty}^{\infty} f(t)\psi_{a_j,b}(t)dt \quad (4)$$

In order to cover the frequency range of earthquake ground motions, j is considered to be -21 to 10 . Additional details about the wavelet transform and time-history decomposition can be found in the literature [17]. The ground motion record, $f(t)$ is assumed to belong to a nonstationary Gaussian process, $F(t)$. This $F(t)$ can be modelled as a Priestley process [18]:

$$F(t) = \int_{-\infty}^{\infty} A(t, \omega) e^{i\omega t} d\bar{Z}(\omega) \quad (5)$$

where, $A(t, \omega)$ is a frequency dependent deterministic slow varying amplitude modulation and $d\bar{Z}(\omega)$ is a stationary orthogonal incremental process. The level-wise instantaneous energy arrival of the wavelet coefficients, $W_{\psi}f(a_j, b)$, can be expressed by

$$E'_j(b) = \int_{-\infty}^b [W_{\psi}f(a_j, \xi)]^2 d\xi \quad (6)$$

From the smooth trend of $E'_j(b)$, denoted by $\bar{E}'_j(b)$, the frequency-dependent modulation (of the underlying Priestley process) for the wavelet coefficient process can be extracted as

$$V'_j(b) = \gamma'_j \left[\left(\frac{d\bar{E}'_j(b)}{db} \right)_N \right]^{\frac{1}{2}} \quad (7)$$

where γ'_j is a level-dependent constant and $(.)_N$ denotes the normalized value of $(.)$ such that the maximum ordinate is unity. From the knowledge of $V'_j(b)$ various samples of the wavelet coefficients are generated from different samples of narrow-band (corresponding to the levels) Gaussian signals. From the samples of wavelet coefficients, thus obtained, the samples of ground motions are obtained by inverse wavelet transform.

2.2 Ground Motion Simulation in Time-Domain

In the present study, any recorded sample, $f(t)$, of a ground motion process, $\mathbf{F}(t)$, is decomposed into 32 different disjoint frequency bands in accordance with 32 levels of wavelet coefficients discussed above. Each



decomposed time-history, denoted by $f_j(t)$, has very similar nonstationary behaviour as exhibited by the corresponding $W_\psi f(a_j, b)$. E.g., Figure 1 shows the decomposed time-histories and the wavelet coefficients for $j = -8$ and 2 for TOT station record during 1995 Kobe Earthquake. It is evident from the figure that the nature of the amplitude modulation of a decomposed time-history is same as that of the corresponding wavelet coefficients within the total duration of the motion. Further, the decomposed motions can be fast obtained by Fourier analysis as [19].

$$f_j(t) = \frac{1}{2\pi} \int_{-\sigma\pi/a_j}^{-\pi/a_j} F(\omega) e^{i\omega t} d\omega + \frac{1}{2\pi} \int_{\pi/a_j}^{\sigma\pi/a_j} F(\omega) e^{i\omega t} d\omega \quad (8)$$

where, $F(\omega) = \int_{-\infty}^{\infty} f(t) e^{-i\omega t} dt$ is the Fourier transform of the recorded signal $f(t)$. In the present work the process-specific simulation method as in [7] is shifted verbatim to the decomposed time-history (i.e. $f_j(t)$) from the wavelet coefficients (i.e. $W_\psi f(a_j, b)$). Hence, the deterministic frequency-dependent slow varying modulation is obtained from the smoothed FDIEAs for $f(t)$ as

$$V_j(t) = \gamma_j \left[\left(\frac{d\bar{E}_j(t)}{dt} \right)_N \right]^{\frac{1}{2}} \quad (9)$$

where,

$$E_j(t) = \int_{-\infty}^t [f_j(\xi)]^2 d\xi \quad \forall j \quad (10)$$

is the FDIEA, $\bar{E}_j(t)$ is the smooth trend of $E_j(t)$. For the levels $j = 7, 8, 9, 10$, $V_j(t)$ is expressed as

$$V_j(t) = \gamma_j \quad (11)$$

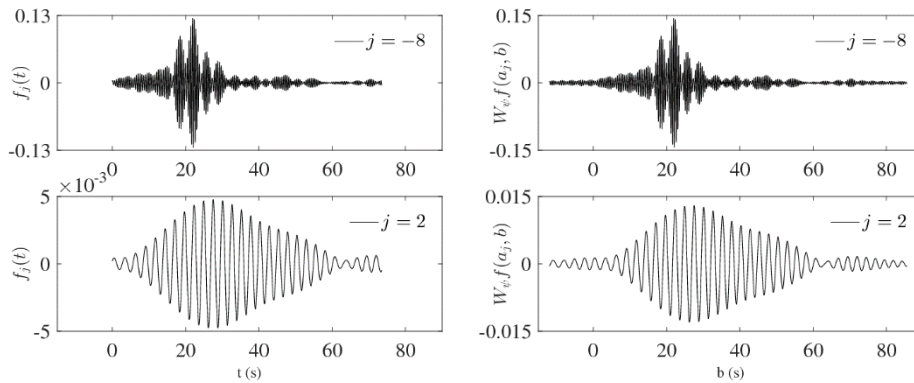


Figure 1 Decomposed time-histories $f_j(t)$ and wavelet coefficients $W_\psi f(a_j, b)$ in the case of TOT station record during 1995 Kobe earthquake for different levels j

This is because at these levels the dominant periods are large enough not to allow proper extraction of the modulations within the recorded duration of the motion [20], so it is assumed to be constant. The contribution of the combined energy from these levels to the total energy of the ground motion is too less to affect the nonstationary features of the reconstructed motion. $V_j(t)$ s are used to modulate samples of a random Gaussian bandlimited process of specific stationary power spectral density function (PSDF) in order to get random samples of $\mathbf{F}(t)$. The values of γ_j s are not required because every generated random sample of $\mathbf{F}(t)$ is scaled such that its total energy is same as that of $f(t)$, level-wise.



From the FDIEA of decomposed motions of the recorded motion considered in Figure 1, 200 samples of ground motions are simulated. Pseudo spectral acceleration (PSA) spectra for 5% damping ratio of the 200 ground motion samples are computed. 5, 50 and 95 percentiles and minimum and maximum spectra and the PSA spectrum of the recorded motion are shown in Figure 2. It can be observed that the minimum and maximum levels of response are able to capture the recorded trend quite satisfactorily. The recorded motion and two simulated random samples are shown in Figure 3. It is clear from the figure that the temporal features of random samples have adequate variability such that neither they look identical nor they look completely different from the recorded signal.

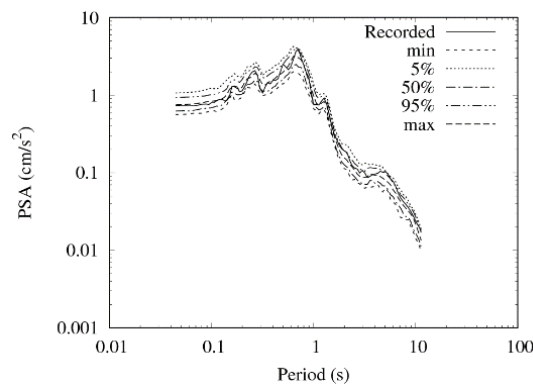


Figure 2 Recorded PSA spectrum along with PSA spectra for different levels of confidence from simulation

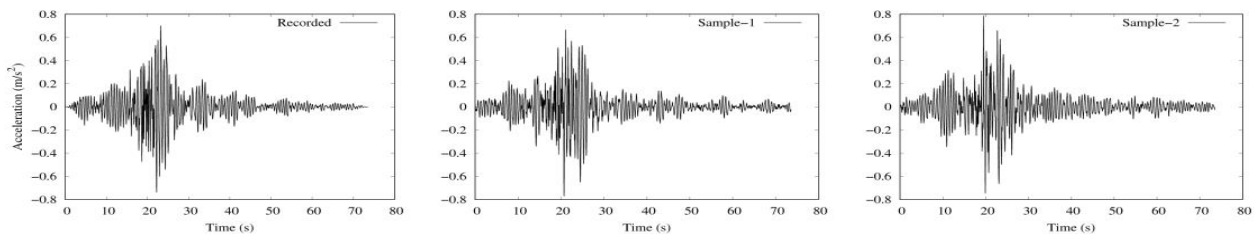


Figure 3 Comparison of recorded motion at TOT station for 1995 Kobe earthquake and two random samples

3. Energy Arrival Scaling Model for Aftershocks

An earthquake scenario-specific ensemble of ground motions can be simulated via FDIEA curves and through a scaling model of the energy arrival curves with respect to different seismological parameters that define the scenario [7]. In an earlier study, Das and Gupta [8] showed that the scaling models for response spectrum and strong motion duration can be modified to develop conditional scaling models for the respective quantities exclusively for the aftershocks. Such scaling models use the actual information of the preceding main shock to predict target quantities for the future aftershocks for an anticipated aftershock scenario. Since FDIEA curves carry the complete information (temporal and spectral) of the ground motion, it is apt to develop a conditional scaling model from the unconditional scaling model of the energy arrival curves. This will enable anyone to simulate samples of aftershock ground motions with desired variability from the knowledge of the preceding main shock for an assumed seismic scenario for the aftershock.

It is possible, finally to arrive at a conditional scaling model for a quantity from an acceptable form of unconditional scaling model for the same quantity [8]. From the knowledge of the basic form of a scaling model for the energy arrival curves [7], a conditional scaling model for the smoothed FDIEA of aftershocks, $\bar{E}_{Aft,j}$, in terms of $a_j(t)$ (ratio of energy arrival of aftershock to that of main shock up to time t for level j) is considered as



$$\ln(\alpha_j(t)) = \ln\left(\frac{\bar{E}_{Aft,j}}{\bar{E}_{Main,j}}\right) = a_{1,j}(t)\Delta M + a_{2,j}(t) \ln\left(\frac{\Delta_{Main}}{\Delta_{Aft}}\right) + a_{3,j}(t)\Delta h; \forall j \quad (12)$$

where, $\bar{E}_{Main,j}(t)$ is the smoothed energy arrival of decomposed motions of main shock, $\Delta M (= M_{Main} - M_{Aft})$ is the difference between main shock and aftershock magnitudes, Δ_{Main} and Δ_{Aft} are representative source-to-site distances (due to Trifunac and Lee [21,22]) of main shock and aftershock respectively, $\Delta h (= h_{Main} - h_{Aft})$ is the difference between main shock and aftershock focal depths. The representative distance Δ takes the finite source dimension into account and in general depends on M , epicentral distance (R), focal depth (h), time period of seismic wave and shear wave velocity of local site (180 m/s, 270 m/s, 850 m/s for the indicator parameter $S = 0, 1$ and 2 , respectively). $a_{1,j}(t)$ takes into account change in energy arrival due to the magnitude difference. $a_{2,j}(t)$ reflects the change in energy arrival because of different geometrical spreading of seismic waves due to difference in representative distances of main shock and aftershock. $a_{3,j}(t)$ accounts for change in energy arrival due to difference in focal depths of main shock and aftershock. The database for the regression analysis comprises north-south component of main shock (93 number of recordings) and aftershock of magnitude 5 and above (394 number of recordings) during the 1999 Chi-Chi earthquake [23,24]. These aftershock records are chosen such that their epicentral distances are within 50 km [8]. Since different motions are having different lengths of record, in order to maintain uniformity, the maximum value of t for evaluation of energy arrival is considered as 70 s. It is understood that any shorter record will reach its 100% energy arrival for a smaller value to t than a longer record. For regression analysis t is discretized every 0.02 s of interval. Maximum likelihood method [25] is used to carry out the regression analysis and the error, $\varepsilon_j(t)$, in the scaling model is defined as

$$\varepsilon_j(t) = \ln(\bar{\alpha}_j(t)) - \ln(\hat{\alpha}_j(t)); \forall j \quad (13)$$

where, $\hat{\alpha}_j(t)$ is the estimated ratio of energy arrival of aftershock to that of main shock using Eq.(12) via estimated smoothed regression coefficients. Further, $\varepsilon_j(t)$ is a normal variate with mean zero and standard deviation $\sigma_j(t)$. It should be mentioned here that for $j=7$ to 10, the regression analysis has been performed only for $t = 70$ s, i.e. only for the 100% energy arrival because the normalized shape of modulations for these levels are constant.

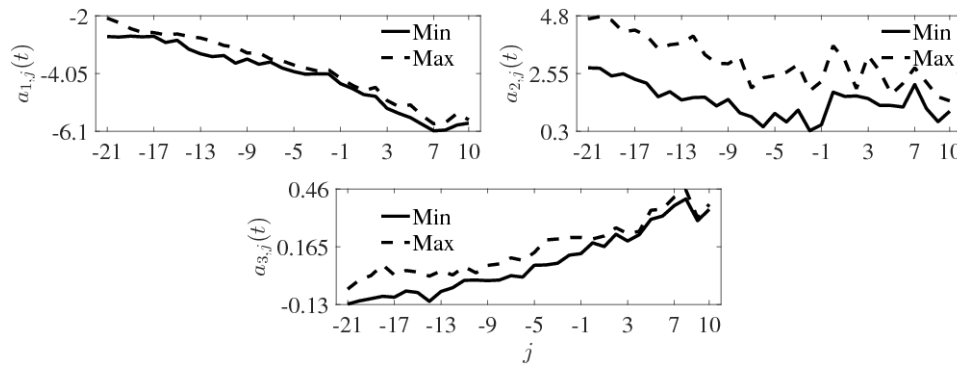


Figure 4 Minimum and maximum values of regression coefficients for $\ln(\hat{E}_{Aft,j}(t))$ as in Equation (12) for different levels, j

To understand the variation of the coefficients with respect to different levels, the maximum and minimum values of all the coefficients along time are shown in Figure 4 for different levels, j . It can be seen from the figure that $a_{1,j}(t)$ is negative for all values of j and t . Negative values of $a_{1,j}(t)$ indicate that smaller



aftershocks will have smaller energy arrival as compared to larger aftershocks, which is meaningful. The magnitude of $a_{1,j}(t)$ is higher at longer periods (higher j s) as larger earthquake event has relatively stronger long period waves compared to smaller event. $a_{2,j}(t)$ is found to be positive throughout since nearer aftershocks will be stronger than farther aftershocks. Also, magnitude of $a_{2,j}(t)$ increases towards shorter periods (smaller j s) as high-frequency waves attenuate faster with distance than the low frequency waves. $a_{3,j}(t)$ is found to be positive for most of the levels since shallower events appear to be stronger. But, $a_{3,j}(t)$ follows a decreasing trend from higher to lower levels because deeper events are expected to have relatively higher proportion of higher frequency waves. Since the Chi-Chi earthquake was a crustal event, the effect of focal depth was not so prominent but still the coefficient $a_{3,j}(t)$ is retained as it reflects the proper trend.

5. Generation of Ensemble of Aftershocks

The proposed conditional scaling model gives the conditional estimate for the FDIEA curves for the aftershock, using which samples of aftershock can be simulated. The statistical description of error in the energy arrival estimation is characterized by a single parameter, $\sigma_j(t)$, the level-wise standard deviation of $\varepsilon_j(t)$. The p th sample for the level-wise energy arrival for a given recorded main shock and scenario of the aftershock can be modelled as [7].

$$\ln(\hat{E}_{\text{Aft},p,j}(t)) = \ln(\hat{E}_{\text{Aft},j}(t)) + k_p \sigma_j(t); \forall j \quad (14)$$

where $\hat{E}_{\text{Aft},j}(t)$ is the estimated (median) energy arrival curve for aftershock corresponding to $\hat{\alpha}_j(t)$ and k_p is a standard normal variate to account for the aleatory uncertainty. For the purpose of scenario-specific ensemble, only one aftershock ground motion is generated randomly from the p th estimated energy arrival curves ($\hat{E}_{\text{Aft},p,j}(t)$) using the process-specific simulation technique as in Section 2.2. This is done because the variation of ground motion samples resulting from different k_p s is much more than the variation of samples within a process (specific to p). It will be interesting to see if the samples generated by the above method can represent the expected trend with variation in the seismological parameters in terms of pseudo spectral velocity (PSV) spectra obtained from the simulated motions. For this purpose, a main shock recording of the Chi-Chi earthquake at C046 station is considered arbitrarily and aftershock ensembles (500 motions for each scenario) are generated for different hypothetical scenarios - Scenario-1 ($M = 5.5, R = 20.0 \text{ km}, h = 2.0 \text{ km}$), Scenario-2 ($M = 6.0, R = 20.0 \text{ km}, h = 2.0 \text{ km}$), Scenario-3 ($M = 6.5, R = 20.0 \text{ km}, h = 2.0 \text{ km}$), Scenario-4 ($M = 6.0, R = 10.0 \text{ km}, h = 2.0 \text{ km}$), Scenario-5 ($M = 6.0, R = 40.0 \text{ km}, h = 2.0 \text{ km}$), Scenario-6 ($M = 6.0, R = 20.0 \text{ km}, h = 8.0 \text{ km}$) and Scenario-7 ($M = 6.0, R = 20.0 \text{ km}, h = 14.0 \text{ km}$). The values of seismological parameters considered for the different seismic scenarios are within the range of values of the seismological parameters of recorded data used for regression analysis. From the simulated ensemble of aftershocks, median Pseudo spectral velocity (PSV) spectra are calculated for the different scenarios. Figure 5 shows a comparative plot of the median PSV spectra with a single seismological parameter varying while keeping others constant. Figure 5(a) shows the median PSV spectra for varying magnitudes (Scenario-1, 2 and 3). The spectral ordinates of larger aftershocks are greater than that of smaller aftershocks, which is observed in Figure 5(a). The difference between spectral ordinates of larger aftershock and smaller aftershock is more in the longer period since a larger aftershock (or any event) has stronger long period waves compared with a smaller aftershock. Figure 5(b) shows the median PSV spectra for varying epicentral distances (Scenario-4, 2 and 5). The strength of ground motions decrease with increase in source to site distance which is observed in Figure 5(b). Figure 5(c) shows the median PSV spectra for varying focal depths (Scenario-2, 6 and 7). It is clear from the figure that deeper events generates weaker long period waves as the source to site distance increases, however this effect is neutralized at the high frequency side because relatively deeper events likely to produce stronger high frequency waves than shallower events.

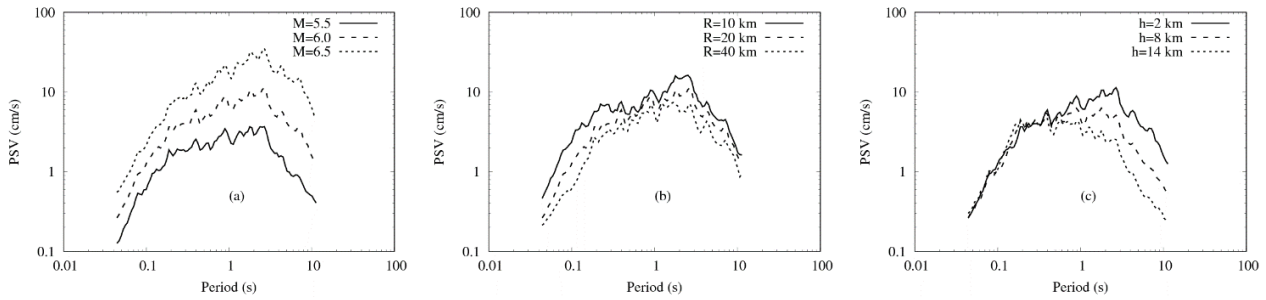


Figure 5 Median PSV spectra of simulated aftershocks for different values of (a) magnitude, (b) distance and (c) depth, when the main shock time-history is same as the Chi-Chi record at station C046

To see the performance of aftershocks simulation with respect to recorded aftershocks, ground motions are generated for some recorded scenarios and the median PSV spectrum is compared with that of the recorded aftershock PSV spectrum. Two recorded aftershock scenarios are arbitrarily considered for this purpose. Figure 6 shows Aft-2146 (aftershock of $M_L = 6.59$ that occurred at 21:46 hrs on September 20) recorded at station C039 and Aft-0014 (aftershock of $M_L = 6.80$ that occurred at 00:14 hrs on September 22) recorded at station H031 for the Chi-Chi earthquake. In each of these figures, PSV spectrum of the main shock ground motion whose energy arrival curves are used to simulate the aftershocks is also shown. The median PSV spectrum of the simulated aftershock ensemble is closer to the recorded aftershock PSV spectrum. It is also interesting to see whether a conditional PSV scaling model obtained from the same database will yield similar results as envisaged by the conditional energy arrival scaling model since the latter is a very different quantity from the PSV. The regression coefficients of the PSV scaling model is obtained using the maximum likelihood method [25], and the mathematical form of the scaling model is chosen as

$$\ln(\beta(T)) = \ln\left(\frac{PSV_{Aft}(T)}{PSV_{Main}(T)}\right) = c_1(T)\Delta M + c_2(T)\ln\left(\frac{\Delta_{Main}}{\Delta_{Aft}}\right) + c_3(T)\Delta h \quad (15)$$

through the same independent parameters as considered for modelling $\alpha_j(t)$. The error in estimation of the scaling model is defined as

$$\varepsilon_\beta(T) = \ln(\beta(T)) - \ln(\hat{\beta}(T)) \quad (16)$$

where, $\ln(\hat{\beta}(T))$ is the estimated ratio of PSV using Eq. (15) through estimated smooth regression coefficients. Further, $\varepsilon_\beta(T)$ is normal variate with mean zero and standard deviation $\sigma_\beta(T)$. In Figure 6, the median PSV spectrum of the PSV scaling model is found to be similar to that of the median PSV spectrum of the simulated aftershock ensemble for two different recorded scenarios. The variation in the temporal features of simulated ground motions is shown by three arbitrarily selected random samples for Aft-1940 (aftershock of $M_L = 5.28$ that occurred at 19:40 hrs on September 20) recorded at station C036 in Figure 7. The variations of the time-frequency characteristics among samples are coming from two facts, viz., a sample represents any random process from the entire pool of random processes the scenario might represent and there is sample to sample variation within a process. The recorded ground motion is also shown in order to show that the recorded motion might very well be a member of the sample space.

The scaling model of energy arrival curves developed by Nithin et al. [7] (hereafter, referred as unconditional scaling model) can be used for the simulation of ground motions for any aftershock scenario but it cannot adequately address the main shock aftershock dependence once the main shock is given. A comparative study of conditional and unconditional simulation is done to clearly demonstrate the necessity for a conditional scaling model for aftershocks. To make the comparison between conditional and unconditional scaling models fair enough, a new form for unconditional scaling model is developed. For this purpose, we consider a form with all the seismological parameters considered while developing the conditional scaling model. Hence, the unconditional model has been considered as

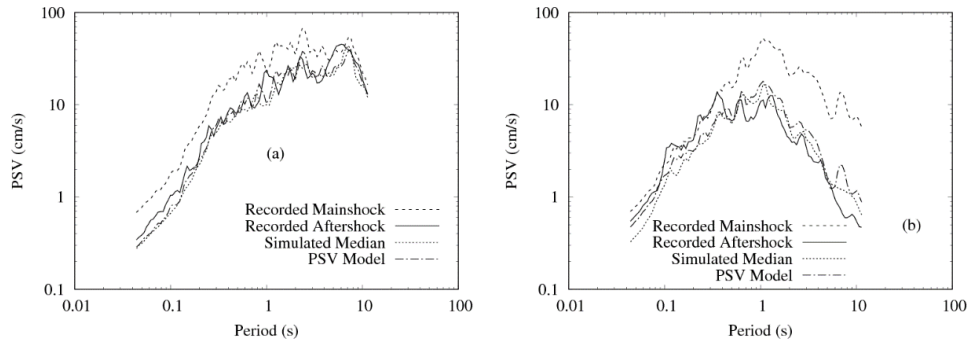


Figure 6 Comparison of the recorded and the median aftershock spectra obtained from both simulated ensemble and the conditional PSV scaling model in the cases of (a) Aft-2146 recorded at station C039 ($M_L = 6.59$, $R = 48.69$ km, $h = 1.05$ km, $S = 1$), (b) Aft-0014 recorded at station H031 ($M_L = 6.80$, $R = 45.82$ km, $h = 15.59$ km, $S = 0$)

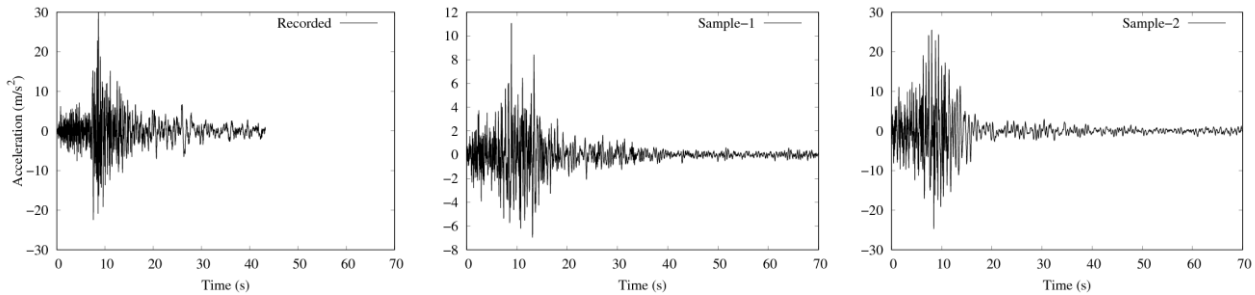


Figure 7 Recorded ground motion and some arbitrarily selected random simulated ground motion samples for Aft-1940 at station C036 ($M_L = 5.28$, $R = 40.97$ km, $h = 7.40$ km, $S = 1$)

$$\ln \bar{E}_j(t) = b_{1,j}M + b_{2,j}(t) \ln \Delta + b_{3,j}(t)h + b_{4,j}(t)S + b_{5,j}(t); \forall j \quad (17)$$

Using the currently developed unconditional and conditional scaling models, ground motions are simulated for some arbitrarily selected scenarios of recorded aftershocks – Aft-2146 recorded at station C014 and Aft-1803 (aftershock of $M_L = 6.60$ that occurred at 18:03 hrs on September 20) recorded at station C029. 200 numbers of ground motions for each case are simulated for the comparative study. Figure 8 shows 10 percentile and 90 percentile PSV spectra of ground motions simulated using conditional and unconditional scaling models and the recorded PSV spectrum. The 10 percentile and 90 percentile spectra of the ground motions simulated by the conditional scaling model are able to capture the trend of the recorded PSV spectrum and follow the trend of the recorded PSV spectrum very well along different time-periods. But the unconditional scaling model is not able to capture the trend of the recorded PSV spectrum along different time-periods and the recorded PSV spectrum lies outside the bound of 10 percentile and 90 percentile for some time-periods, this observation is for other various scenarios especially for larger aftershocks. Figure 9 shows the percentage of records for which the recorded PSV spectral ordinates lie within 10 and 90 percentile PSV spectra (from 200 samples every case) of motions simulated by conditional and unconditional scaling models separately for larger and smaller aftershocks. For $M_L > 6.0$, the performance of conditional model is similar to that of the unconditional model till time-period of 1.0s and afterwards conditional model performs much better than the unconditional model. Since time-period of a damaged structure (during main shock) increases, better estimation towards longer period improves accuracy in larger aftershock induced additional vulnerability. For $M_L < 6.0$, the improvement of conditional scaling model is relatively less as compared to the improvement seen for the larger aftershocks at longer periods, but the same level of improvement is seen



along all periods. The improvement even in the shorter period range for smaller aftershocks (not seen in the case of larger aftershocks) may arise from the fact that smaller aftershocks are relatively rich in high frequency content so the conditional model helps to improve upon in that range.

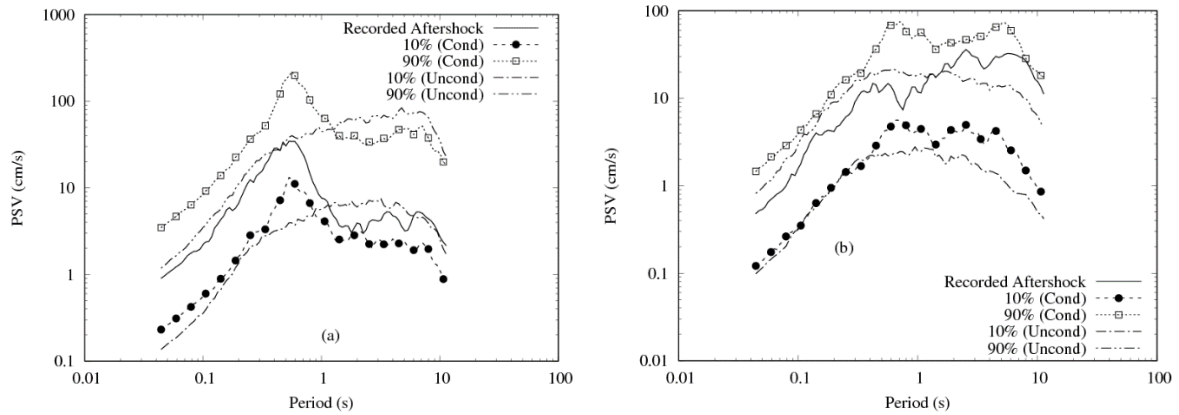


Figure 8 Recorded PSV spectrum and 10 and 90 percentile PSV spectra of ground motions simulated using conditional and unconditional scaling models for (a) Aft-2146 at station C014 ($M_L = 6.59$, $R = 42.07$ km, $h = 1.05$ km, $S = 1$), (b) Aft-1803 at station C029 ($M_L = 6.60$, $R = 40.27$ km, $h = 8.19$ km, $S = 2$)

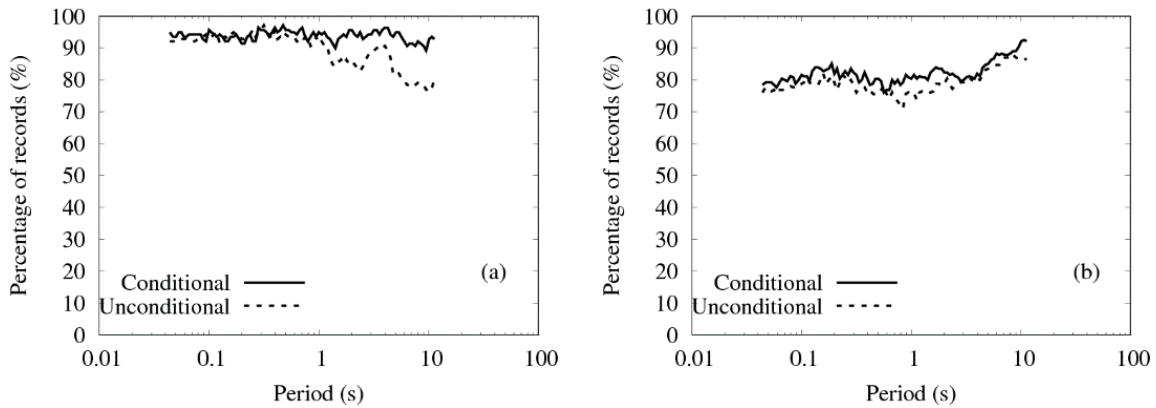


Figure 9 Spectra of percentage of cases wherein the recorded PSV ordinates lie within 10 and 90 percentile PSV spectra of simulated motions in the cases of recorded scenarios (a) with $M_L \geq 6.0$, (b) with $M_L < 6.0$

Table 1 Comparison of the observed SMD (in s) with statistical estimates of SMD (in s) from the simulated samples generated using the conditional and unconditional scaling models

Event Name	Station Name	Observed	Confidence Probability Levels					
			Conditional			Unconditional		
			Median	10%	90%	Median	10%	90%
Aft-2146	C028	12.47	12.59	9.45	15.77	21.01	15.61	26.83
Aft-2002	T140	32.21	31.47	29.72	32.58	23.88	18.92	25.33



Other than the response spectrum the SMD also plays important role in cumulative damage during any aftershock event. For that purpose the statistics of SMD obtained from simulated ground motions from both conditional and unconditional scaling models are presented for two records arbitrarily chosen. Table 1 shows the comparison in the cases of Aft-2146 recorded at station C028 and Aft-2002 (aftershock of $M_L = 5.35$ that occurred at 20:02 hrs on September 20) recorded at station T140. It is clear that the conditional scaling model can predict the SMD better than the unconditional one. The results in Figs. 6–8 and Table 1 collectively demonstrate the effectiveness of the conditional scaling model in capturing the trends of recording scenarios.

5. Conclusions

In the present study, a previous ground motion simulation method has been shifted from wavelet-domain to time-domain for faster simulation of ground motions. A conditional scaling model for aftershocks has been proposed where the energy arrival curves of an aftershock are predicted conditionally from those of the preceding main shock motion with known seismic scenarios for both main shock and the aftershock. Finally the scenario-specific and conditional ground motion samples of the aftershock have been simulated from the frequency-dependent modulations (obtained from the predicted energy arrival curves), which are fully nonstationary by nature. The major contributions and conclusions of the current study are listed below.

- An earthquake recording process-specific simulation technique proposed by Nithin et al. [7] has been improved by shifting from the wavelet domain to the time domain for faster simulation. The new technique yields similar simulated motions as obtained from the previous wavelet-based approach.
- A conditional scaling model for aftershock has been proposed to predict the FDIEA from that of the preceding main shock in terms of the disparities of various seismological parameters. The simulated ground motions using the conditional scaling model show expected trend vis-à-vis the seismological scenarios in terms of the PSV spectra obtained from them.
- The conditional scaling model has been found to perform better than the unconditional scaling model in capturing the recorded response spectra through the 10 and 90 percentile PSV spectra and SMD of simulated motions.

6. References

- [1] O. C. Celik, B. R. Ellingwood, Seismic fragilities for non-ductile reinforced concrete frames - Role of aleatoric and epistemic uncertainties, *Structural Safety* 32 (1) (2010) 1-12.
- [2] Y. C. Kurama, K. T. Farrow, Ground motion scaling methods for different site conditions and structure characteristics, *Earthquake Engineering & Structural Dynamics* 32 (15) (2003) 2425-2450.
- [3] F. Naeim, A. Alimoradi, S. Pezeshk, Selection and scaling of ground motion time histories for structural design using genetic algorithms, *Earthquake Spectra* 20 (2) (2004) 413-426.
- [4] Y. N. Huang, A. S. Whittaker, N. Luco, R. O. Hamburger, Scaling earthquake ground motions for performance-based assessment of buildings, *Journal of Structural Engineering* 137 (3) (2011) 311-321.
- [5] Y. Yamamoto, J.W. Baker, Stochastic model for earthquake ground motion using wavelet packets, *Bulletin of the Seismological Society of America* 103 (6) (2013) 3044-3056.
- [6] S. Rezaeian, A. Der Kiureghian, Simulation of synthetic ground motions for specified earthquake and site characteristics, *Earthquake Engineering and Structural Dynamics* 39 (10) (2010) 1155-1180.
- [7] V. L. Nithin, S. Das, H. B. Kaushik, Wavelet-based simulation of scenario-specific nonstationary accelerograms and their GMPE compatibility, *Soil Dynamics and Earthquake Engineering* 99 (2017) 56-67.



- [8] S. Das, V. K. Gupta, Scaling of response spectrum and duration for aftershocks, *Soil Dynamics and Earthquake Engineering* 30 (8) (2010) 724-735.
- [9] S. Hainzl, A. Christophersen, D. Rhoades, D. Harte, Statistical estimation of the duration of aftershock sequences, *Geophysical Journal International* 205 (2) (2016) 1180-1189.
- [10] A. N. Papadopoulos, M. Kohrangi, P. Bazzurro, Correlation of spectral acceleration values of mainshock-aftershock ground motion pairs, *Earthquake Spectra* 35 (1) (2019) 39-60.
- [11] K. Goda, C. A. Taylor, Effects of aftershocks on peak ductility demand due to strong ground motion records from shallow crustal earthquakes, *Earthquake Engineering & Structural Dynamics* 41 (15) (2012) 2311-2330.
- [12] K. Goda, Record selection for aftershock incremental dynamic analysis, *Earthquake Engineering & Structural Dynamics* 44 (7) (2015) 1157-1162.
- [13] J. P. Conte, B. F. Peng, Fully nonstationary analytical earthquake ground motion model, *Journal of Engineering Mechanics* 123 (1) (1997) 15-24.
- [14] L. Peng, G. Huang, X. Chen, Q. Yang, Evolutionary spectra-based time varying coherence function and application in structural response analysis to downburst winds, *Journal of Structural Engineering* 144 (7).
- [15] S. Hu, P. Gardoni, L. Xu, Stochastic procedure for the simulation of synthetic main shock-aftershock ground motion sequences, *Earthquake Engineering & Structural Dynamics* 47 (11) (2018) 2275-2296.
- [16] S. Das, V. K. Gupta, Wavelet-based simulation of spectrum-compatible aftershock accelerograms, *Earthquake Engineering and Structural Dynamics* 37 (11) (2008) 1333-1348.
- [17] B. Basu, V. K. Gupta, Seismic response of SDOF systems by wavelet modelling of nonstationary processes, *Journal of Engineering Mechanics* 124 (10) (1998) 1142-1150.
- [18] M. B. Priestley, Evolutionary spectra and non-stationary processes, *Journal of the Royal Statistical Society. Series B (Methodological)* (1965) 204-237.
- [19] S. Das, B. Hazra, Frequency-dependent principal component analysis of multicomponent earthquake ground motions, *Earthquake Engineering & Structural Dynamics* 47 (5) (2018) 1360-1366.
- [20] S. Das, V. K. Gupta, A wavelet-based parametric characterization of temporal features of earthquake accelerograms, *Engineering Structures* 33 (7) (2011) 2173-2185.
- [21] M. D. Trifunac, V. W. Lee, Frequency dependent attenuation of strong earthquake ground motion, *Soil Dynamics and Earthquake Engineering* 9 (1) (1990) 3-15.
- [22] M. D. Trifunac, V. W. Lee, Empirical models for scaling pseudo relative velocity spectra of strong earthquake accelerations in terms of magnitude, distance, site intensity and recording site conditions, *Soil Dynamics and Earthquake Engineering* 8 (3) (1989) 126-144.
- [23] W. H. K. Lee, T. C. Shin, C. F. Wu, CWB free-field strong-motion data from 30 early aftershocks of the 1999 Chi-Chi earthquake: Processed acceleration data files on CD-ROM, CWB strong-motion data series CD-003, Seismological Observation Center of Central Weather Bureau: Taipei, Taiwan, 2001.
- [24] W. H. K. Lee, T. C. Shin, C. F. Wu, CWB free-field strong-motion data from three major aftershocks of the 1999 Chi-Chi earthquake: Processed acceleration data files on CD-ROM, CWB strong-motion data series CD-002, Seismological Observation Center of Central Weather Bureau: Taipei, Taiwan, 2001.
- [25] W. B. Joyner, D. M. Boore, Methods for regression analysis of strongmotion data, *Bulletin of the Seismological Society of America* 83 (2) (1993) 469-487.